The escape of ionizing photons from supernova-dominated primordial galaxies

Hidenobu Yajima^{1*}, Masayuki Umemura¹, Masao Mori¹, and Taishi Nakamoto²
¹Center for Computational Sciences, University of Tsukuba, Tsukuba 305-8577, Japan

- ² Earth and Planetary Sciences, Tokyo Institute of Technology, 2-12-1 Ookayama, Meguro-ku, Tokyo, 152-8551, Japan

Accepted ?; Received ??; in original form ???

ABSTRACT

In order to assess the contribution of Lyman break galaxies (LBGs) and Lyman alpha emitters (LAEs) at redshifts 3 < z < 7 to the ionization of intergalactic medium (IGM), we investigate the escape fractions of ionizing photons from supernovadominated primordial galaxies by solving the three-dimensional radiative transfer. The model galaxy is employed from an ultra-high-resolution chemodynamic simulation of a primordial galaxy by Mori & Umemura (2006), which well reproduces the observed properties of LAEs and LBGs. The total mass of model galaxy is $10^{11} M_{\odot}$. We solve not only photo-ionization but also collisional ionization by shocks. In addition, according to the chemical enrichment, we incorporate the effect of dust extinction, taking the size distributions of dust into account. As a result, we find that dust extinction reduces the escape fractions by a factor 1.5 - 8.5 in the LAE phase and by a factor 2.5-11 in the LBG phase, while the collisional ionization by shocks increases the escape fractions by a factor ≈ 2 . The resultant escape fractions are 0.07-0.47 in the LAE phase and 0.06 - 0.17 in the LBG phase. These results are well concordant with the recent estimations derived from the flux ratio at 1500 Å to 900 Å of LAEs and LBGs. Combining the resultant escape fractions with the luminosity functions of LAEs and LBGs, we find that high-z LAEs and LBGs can ionize the IGM at z = 3-5. However, ionizing radiation from LAEs as well as LBGs falls short to ionize the IGM at z > 6. That implies that additional ionization sources may required at z > 6.

Key words: radiative transfer – ISM: dust, extinction – galaxies: evolution – galaxies: formation – galaxies: high-redshift

INTRODUCTION

One of momentous issues regarding the evolution of intergalactic medium (IGM) is the ionization history of the universe, which significantly influences the galaxy formation (e.g., Susa & Umemura 2000; Umemura, Nakamoto, & Susa 2001; Susa & Umemura 2004). The Wilkinson Microwave Anisotropy Probe (WMAP) results provide a wealth of information about the cosmic reionization (Page et al. 2007; Dunkley et al. 2009). However, the detailed history of reionization and the nature of ionizing sources are not yet fully understood. Haardt & Madau (1996) pointed out that the UV background radiation is dominated by quasars at z < 4. Fan et al. (2001) showed, using the SDSS sample, that the bright-end slope of the quasar luminosity function at $z \gtrsim 4$

are considerably shallower than that at low-redshifts, and they concluded that quasars cannot maintain the ionization of IGM at $z \gtrsim 4$. Subsequently, a lot of arguments have been concentrated on the possibility that the IGM is ionized mainly by UV radiation from high-z star-forming galaxies like Lyman break galaxies (LBGs) and Lyman α emitters (LAEs) (e.g., Fan et al. 2006; Bouwens et al. 2007; Gnedin 2008). However, the estimate of the contribution of LBGs or LAEs suffers significantly from the ambiguity regarding the escape fractions of ionizing photons from star-forming galaxies (Razoumov & Sommer-Larsen 2006; Gnedin, Kravtsov & Chen 2008).

Observationally, the escape fractions of ionizing photons are assessed by the relative escape fractions $f_{\rm esc,rel}$, using the flux ratio at 1500 Å to 900 Å, $(F1500/F900)_{obs}$, which are defined by

$$f_{\rm esc,rel} = \frac{(L1500/L900)_{\rm int}}{(F1500/F900)_{\rm obs}} \exp(\tau_{900}^{\rm IGM}), \tag{1}$$

2

where $au_{900}^{\rm IGM}$ represents the line-of-sight opacity of the IGM for 900 $\mbox{\normally}$, the intrinsic luminosity ratio at 1500 Å to 900 Å, $(L1500/L900)_{int}$, is assumed to be 3 as a fiducial value. Steidel, Pettini & Adelberger (2001) found $f_{\rm esc,rel} \gtrsim 0.5$ from the composite spectrum of 29 LBGs at $z\,\sim\,3,$ and Giallongo et al. (2002) and Inoue et al. (2005) estimated the upper limit of $f_{\rm esc,rel} \lesssim 0.1-0.4$ for some LBGs at $z \sim 3$. The direct detection of ionizing photons from high-z star-forming galaxies has been accomplished recently as a consequence of intensive and continuous exertion. Shapley et al. (2006) detected the escaping ionizing photons from 2 LBGs in the SSA22 field at z = 3.1 and they estimated the average relative escape fraction $f_{\rm esc,rel} = 0.14$. Moreover, Iwata et al. (2009) successfully detected the Lyman continuum emission from 10 LAEs and 7 LBGs within 197 samples of LAEs and LBGs in the SSA22 field. They have shown that the mean value of relative escape fractions for 7 LBGs is 0.11 after a correction for dust extinction, and can be 0.20 if IGM extinction is taken into account.

Theoretically, the accurate estimation of escape fractions requires the three-dimensional (3D) radiative transfer calculations of ionizing photons traveling in inhomogeneous interstellar medium. Such 3D radiative transfer calculations are fairly recent attempts, because a great deal of computations are demanded. First, Ciardi, Bianchi & Ferrara (2002) calculated the escape fractions in simple model clouds, where the density distributions are smoothed Gaussian or fractally inhomogeneous. More recently, using gasdynamical simulations of galaxy formation, the escape fractions are estimated by solving 3D radiative transfer. Razoumov & Sommer-Larsen (2006, 2007) have found that the escape fractions decline from several per cent at z = 3.6to 0.01-0.02 at z = 2.39, due to higher gas clumping at lower redshifts. But, in these simulations, the effects of dust extinction are not taken into account. Gnedin et al. (2008) performed a cosmological simulation on the formation of a disk-like galaxy that provides the three-dimensional distributions of absorbing gas in and around the galaxy. Then, 3D radiative transfer was solved including the dust extinction. As a result, the escape fractions turned out to be as low as a few per cent. In this model, the bulk of stars is embedded deep inside the optically-thick HI disk and therefore most of ionizing photons emitted from hot stars are absorbed by neutral hydrogen in the HI disk. Only a small fraction of ionizing photons from the stars that are located near the edge of disk can escape from the galaxy. Hence, almost regardless of the effects of dust extinction, the resultant escape fractions become quite small. It implies that star-forming galaxies cannot give a significant contribution to the IGM ionization at $z \gtrsim 3$. For higher redshift $z \gtrsim 8$, on the other hand, some numerical simulations have already shown that large escape fractions of some tens per cent are possible for low-mass galaxies, which include Pop III stars (Alvarez, Bromm & Shapiro 2006; Whalen et al. 2004; Kitayama et al. 2004; Wise & Cen 2009). However, in order to assess the contribution of LAEs and LBGs observed at $3 \lesssim z \lesssim 7$ to IGM reionization, we should evaluate the UV escape fractions from more massive galaxies. The escape of UV photons can sensitively depend on the gravitational potential (Whalen et al. 2004, Kitayama et al. 2004). Also, dust extinction should be taken into account in such primordial galaxies.

In this paper, we reconsider the escape fractions of ionizing photons from high-z primordial galaxies by employing a supernova-dominated primordial galaxy model proposed by Mori & Umemura (2006), which well reproduces the observed properties of LAEs and LBGs. The total mass is $10^{11} M_{\odot}$, and the star formation with the Salpeter IMF is included. In this model, stars are distributed more extendedly in the galaxy and the bulk of interstellar gas is collisionally ionized by supernova-driven shock. The spread of stellar distributions and the shock heating can lead to diminishing the absorption of ionizing photons and may enhance escape fractions. Here, we perform the 3D radiative transfer calculations including not only the photo-heating but also the shock heating. We incorporate the dust extinction that is consistent with the chemical evolution of galaxy. Then, using the resultant escape fractions, we explore whether LAEs and LBGs can contribute to the ionization of IGM in a highz universe. In the present analyses, the cosmological parameters are assumed to be $H_0 = 70 \text{ km s}^{-1} \text{ Mpc}^{-1}$, $\Omega_{\rm M} = 0.3$ and $\Omega_{\Lambda} = 0.7$. In §2, the model and numerical method are described. In §3, the numerical results on escape fractions are provided. In §4, we argue the contributions of LAEs and LBGs to the IGM ionization. In §5 is devoted to the summary.

2 MODEL AND METHOD

As a model galaxy, we adopt the high-resolution hydrodynamic simulations (1024³ fixed Cartesian grids) by Mori & Umemura (2006), which are coupled with the collisionless dynamics for dark matter particles as well as star particles and also the chemical enrichment. The simulation box size is 134 kpc in physical scales. Mori & Umemura (2006) demonstrated that an early proto-galactic evolution with multitudinous type II SNe (SNeII) exhibits intense Lyman α emission, well resembling LAEs. Subsequently, the galaxy shifts to a stellar continuum radiation-dominated phase, which appears like LBGs. In the present analysis, the stages from $t_{\rm age} = 0.1 \, {\rm Gyr}$ to $t_{\rm age} = 0.3 \, {\rm Gyr}$ are defined to be the LAE phase, and the stages from $t_{\rm age} = 0.5 \, {\rm Gyr}$ to $t_{\rm age} = 1.0 \, {\rm Gyr}$ are the LBG phase.

As a post process, we calculate the escape fractions of ionizing photons with an accurate radiation transfer scheme. The data of the hydrodynamic simulations are coarsegrained into 128³ Cartesian grids to solve radiation transfer. We use the Authentic Radiation Transfer method (ART) developed by Nakamoto, Umemura & Susa (2001). The performance of this scheme has already reported as a part of the comparison study by Iliev et al. (2006a). The radiation transfer equation is solved along 128² rays with uniform angular resolution from each source. At a point of optical depth τ , the specific intensity is given by $I_{\nu}(\tau) = I_{\nu}(0) \exp(-\tau)$, where $I_{\nu}(0)$ is the intrinsic intensity of ionizing radiation and τ is the optical depth of neutral hydrogen and dust. As for scattering photons, we employ the on-the-spot approximation (Osterbrock 1989), in which scattering photons are assumed to be absorbed immediately on the spot. We obtain the ionization structure assuming the ionization equilibrium, $\Gamma^{\gamma} n_{\rm HI} + \Gamma^{C} n_{\rm HI} n_{\rm e} = \alpha_{\rm B} n_{\rm p} n_{\rm e}$, where $\Gamma^{\gamma}, \Gamma^{C}$ and $\alpha_{\rm B}$ are the photo-ionization rate, the collisional ionization rate and the recombination rate to all excited states, respectively. We continue the radiative transfer calculation recurrently until the ionization structure converges. In a supernova-dominated model galaxy, the collisional ionization occurs mostly in low density, high temperature regions with $n \lesssim 10^{-3} \text{cm}^{-3}$ and $T_{\text{coll}} > 10^4 \text{K}$. In such regions, stellar UV radiation contributes to the increase of ionization degree, but does not much to the increase of the temperature. On the other hand, neutral regions are photoionized and heated up to $\sim 10^4 \mathrm{K}$ (Umemura & Ikeuchi 1984; Thoul & Weinberg 1996), when ionizing radiation is irradiated. Hence, in the present analysis, we assume the gas temperature to be $T = \max\{T_{\text{coll}}, 10^4 \text{K}\}\$ in ionized regions, and we do not update the temperature in iteration of radiation transfer calculation. To evaluate the escape fraction of ionizing photons, we count all photons above the Lyman limit that escape from the calculation box.

The number of ionizing photons emitted from source stars is computed based on the theoretical spectral energy distribution (SED) given by a population synthesis scheme, PÉGASE v2.0 (Fioc & Rocca-Volmerange 1997). We assume the Salpeter (1955) initial mass function in the mass range of $0.1M_{\odot} - 50M_{\odot}$. As for dust grains, we adopt the empirical size distribution $n_{\rm d}(a_{\rm d}) \propto$ $a_{\rm d}^{-3.5}$ (Mathis, Rumpl & Nordsieck 1977) in the range from $0.1\mu\text{m}$ - $1.0\mu\text{m}$, where $a_{\rm d}$ is the radius of a dust grain. We assume refractory grains like silicates, for which the photodestruction of dust by UV radiation is negligible over the Hubble time-scale (Draine & Salpeter 1979). The dust grains are distributed proportionally to the metallicity calculated in the hydrodynamic simulations with the relation of $m_d = 0.01 m_q(Z/Z_{\odot})$, where m_d , m_q , and Z are the dust mass, gas mass, and metallicity in a grid. The density in a dust grain is assumed to be 3 g cm^{-3} like silicates. The dust opacity is given by $d\tau_{\rm dust} = Q(\nu)\pi a_{\rm d}^2 n_{\rm d} ds$, where $Q(\nu), a_{\rm d}$ and $n_{\rm d}$ are the absorption Q-value, dust size and number density of dust grains, respectively. Since the assumed range of dust size is larger than the wavelength of Lyman limit, we assume $Q(\nu) = 1$ for ionizing photons (Draine & Lee 1984).

3 RESULTS

3.1 Galactic Evolution

Figure 1 shows the snapshots for the evolution of model galaxy as a function of redshift from $t_{\rm age}=0.1$ to 1.0 Gyr. The density of gaseous and stellar components are adopted from Mori & Umemura (2006) . The dust density is evaluated by the metallicity. As a result of multiple supernova explosions, dust is distributed more extendedly than stars, which is significantly relevant to the absorption of ionizing photons. Bottom panels show the calculated ionization structure in terms of neutral hydrogen fractions $\chi_{\rm HI}$.

First, we see the evolution of the model galaxy. At $t_{\rm age}=0.1$ Gyr, stars form in high-density peaks in subgalactic condensations and the burst of star formation starts. Then, massive stars in the star-forming regions explode as SNeII one after another. The gas in the vicinity of SNeII is quickly enriched with the ejected heavy elements and then interstellar dust is locally procreated. However, a large amount of gas still retains a metal-free and dust-free state. The spatial distributions of heavy elements are highly inhomogeneous, where gas enriched with $-5.1 \lesssim [\mathrm{Si}/\mathrm{H}] \lesssim -1.1$

and $-5 \lesssim {\rm [O/H]} \lesssim -1.0$ coexist with virtually metal-free gas. Supernova-driven shocks collide with each other to generate large-scale hot ($\geqslant 10^6$ K) bubbles reaching a higher ionization degree. At $t_{\rm age} = 0.3$ Gyr, roughly 50 per cent of the total volume is highly ionized with $\chi_{\rm HI} = 10^{-6} \sim 10^{-7}$, where the ionization degree is controlled by the collisional ionization by shock heating and the photo-ionization by UV radiation from hot young stars. The spatial distributions of the heavy elements are still highly inhomogeneous in the range of $-2.4 \lesssim {\rm [Si/H]} \lesssim -0.4$ and $-2.5 \lesssim {\rm [O/H]} \lesssim -0.5$.

After $t_{\text{age}} = 0.5$ Gyr, the hot bubbles expand and blow out into the intergalactic space. As a result, more than 80 per cent of volume is occupied with highly ionized gas with $\chi_{\rm HI}=10^{-6}\sim10^{-7}.$ Finally, the merger of sub-galactic condensations promotes the mixing of heavyelements and weakens the spatial inhomogeneities of heavyelement abundance and ionization degree. As a result, the heavy-element abundance of interstellar medium (ISM) converges to $-0.4 \lesssim [\mathrm{Si/H}] \lesssim 0.1$ and $-0.3 \lesssim [\mathrm{O/H}] \lesssim 0.2$ with small dispersion, and eventually 95 per cent of volume is filled with ionized gas. This means that the metallicity reaches around the solar abundance in 10⁹yr. It is consistent with the previous works on the elliptical galaxy formation (Arimoto & Yoshii 1987; Gibson 1997; Kodama & Arimoto 1997; Kawata & Gibson 2003a,b). The mean value of mass weighted heavy-element abundance is $[Si/H] \simeq -1.0$ and $[O/H] \simeq -0.9$ at the LAE phase, while $[Si/H] \simeq -0.4$ and $\mathrm{[O/H]} \simeq -0.3$ at the LBG phase. These are translated into the mass weighted metallicity as $0.14 Z_{\odot}$ at LAE phase and $0.52~Z_{\odot}$ at LBG phase, which are concordant with the observations by Pettini et al. (2001) and Mannucci et al. (2009).

The luminosity of Lyman α emission, which is the cooling radiation by interstellar gas, reaches 2.0×10^{43} erg s⁻¹ at $t_{\rm age} = 0.1$ Gyr and 1.6×10^{43} erg s⁻¹ at $t_{\rm age} = 0.3$ Gyr, respectively. They nicely match the observed luminosity of LAEs and also well resemble LAEs with respect to other properties. After $t_{\rm age} \leq 0.5$ Gyr, the Lyman α luminosity quickly declines to several 10^{41} erg s⁻¹ that is lower than the detection limit. Then, the galaxy shifts to a stellar continuum radiation-dominated phase, which appears like LBGs (see Mori & Umemura 2006).

3.2 Escape Fractions

Figure 2 shows the time evolution of escape fractions of ionizing photons derived by the full radiation transfer calculations. The upper panel represents the absolute escape fractions, which are defined by

$$f_{\rm esc} \equiv \frac{N_{\rm esc}^{\gamma}}{N_{\rm total}^{\gamma}},$$
 (2)

where $N_{\rm total}^{\gamma}$ is the total number of pristine photons radiated from stars and $N_{\rm esc}^{\gamma}$ is the number of photons escaped from the simulation box. Filled circles in the upper panel of Fig. 2 represent the resultant escape fractions $f_{\rm esc}$ with dust extinction. In the LAE phase, $f_{\rm esc}=0.47$ at $t_{\rm age}=0.1$ Gyr and $f_{\rm esc}=0.23$ at $t_{\rm age}=0.3$ Gyr, while in the LBG phase, $f_{\rm esc}=0.19$ at $t_{\rm age}=0.5$ Gyr and $f_{\rm esc}=0.17$ at $t_{\rm age}=1.0$ Gyr. The escape fractions have the dependence on the size distributions of dust, since smaller grains result in lager extinction for a given dust-to-gas ratio. If we extend the range to smaller grains as $0.02-1.0\mu{\rm m}$, the escape

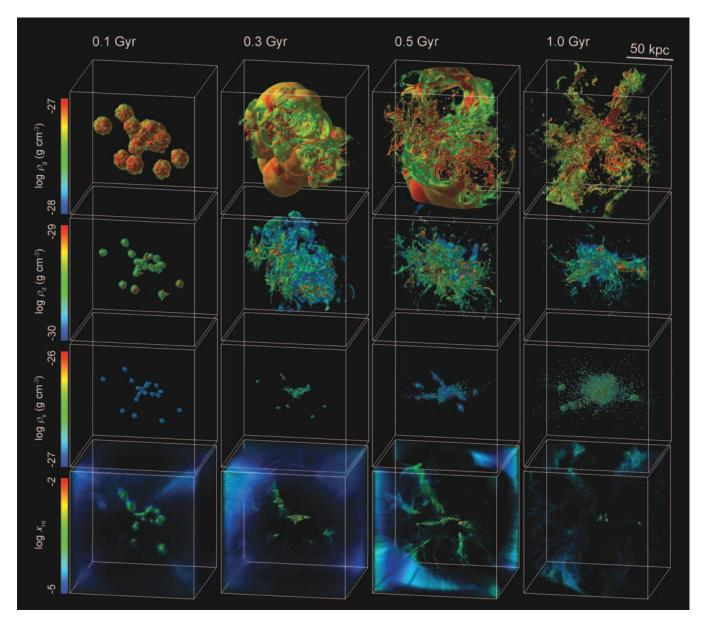


Figure 1. Snapshots of the evolution of the model galaxy with total mass of $10^{11} M_{\odot}$, at $t_{\rm age} = 0.1, 0.3, 0.5$ and 1.0 Gyr. Each panel in row corresponds the spatial distributions of gas density $\rho_{\rm g}$ (g cm⁻³), dust density $\rho_{\rm d}$ (g cm⁻³), stellar density $\rho_{\rm s}$ (g cm⁻³), and fractions of neutral hydrogen in logarithmic scale $\chi_{\rm HI}$, respectively. The simulation box is 134 kpc in physical scale.

fractions are reduced to $f_{\rm esc}=0.1-0.3$ in the LAE phase and $f_{\rm esc}=0.09-0.1$ in the LBG phase. If the grains are even smaller as $0.03-0.3\mu{\rm m}$, the escape fractions become $f_{\rm esc}=0.07-0.22$ in the LAE phase and $f_{\rm esc}=0.06-0.07$ in the LBG phase. These values are concordant with the estimations for LBGs by Shapley et al. (2006) and Iwata et al. (2009).

The escape fractions are significantly regulated by interstellar dust. In Fig. 2, we also show the dust-free model (open circles), where the absorption by interstellar dust is artificially switched off. We find that the dust extinction reduces $f_{\rm esc}$ by a factor of 1.5-8.5 in the LAE phase. On the other hand, The reduction by dust extinction is a factor of 2.5 – 11 in the LBG phase. The change of the reduction factor is linked to the enrichment of heavy elements in the galaxy.

Gnedin et al. (2008) have shown that the escape fractions are as small as a few per cent, which is much smaller than the present results. In the calculations by Gnedin et al. (2008), most of young stars are distributed in the dense region of galactic disk. In our model, stars are extendedly distributed, and also the bulk of interstellar gas is collisionally ionized by the SN shock heating. Since the interstellar medium is moderately optically-thin for ionizing photons, ionizing photons can escape through collisionally-ionized regions. To assess the effects of collisional ionization, we have tentatively calculated a case assuming $T = 10^4 \text{K}$ and no collisional ionization. As a result, we have found that the escape fractions are reduced to be $f_{\rm esc}=0.21$ at $t_{\rm age}=0.1$ Gyr and $f_{\rm esc}=0.13$ at $t_{\rm age}=1.0$ Gyr. This implies that the collisional ionization by shocks can contribute to enhance the escape fractions by a factor of two.

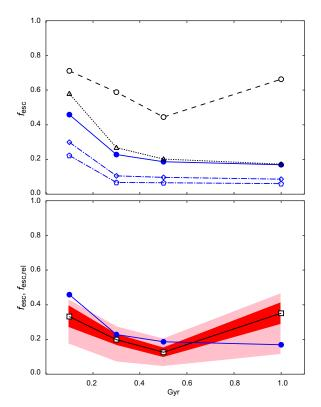


Figure 2. Upper panel: Absolute escape fractions $f_{\rm esc}$ for the simulated galaxy as a function of evolutionary time. Blue symbols represent the escape fractions $f_{\rm esc}$ with dust extinction, where blue filled circles, open diamonds, and open pentagons show the escape fraction for dust size of $0.1-1.0\mu{\rm m},~0.02-1.0\mu{\rm m},~and~0.03-0.3\mu{\rm m},~respectively.$ Black open circles denote $f_{\rm esc}$ without dust extinction. The black open triangles show the dust sputtering model. Lower panel: Absolute escape fractions $f_{\rm esc}$ for dust size of $0.1-1.0\mu{\rm m}$ are compared to relative escape fractions $f_{\rm esc,rel}$ that are derived from the flux ratio at 1500 Å to 900 Å [see equation (1)]. The filled circles represent the absolute escape fractions $f_{\rm esc,rel}$. The variations by viewing angles are represented by a pink belt with the standard deviation shown by a narrower red

If dust grains are in high-temperature regions with $T \gtrsim 10^6 K$, they may be destructed by sputtering process. The grain radius a_d decreases at a rate $da_d/dt =$ $-n_{\rm p}h_{\rm w}[1+(T_{\rm s}/T)^{2.5}]^{-1}~{\rm cm~s^{-1}}~{\rm (Draine~\&~Salpeter~1979;}$ Tsai & Mathews 1995; Mathews & Brighenti 2003), where $h_{\rm w}=3.2\times10^{-18}~{\rm cm^4~s^{-1}}$ and $T_{\rm s}=2\times10^{6}~{\rm K}$ are fitting parameters, and $n_{\rm p}$ is the proton number density. Therefore, the destruction time scale of $\sim 0.1~\mu$ m dust is shorter than the time scale of galaxy evolution ($\lesssim 1 \text{Gyr}$), if $n_{\rm p} \gtrsim 10^{-4}~{\rm cm}^{-3}$ and $T \gtrsim 10^6~{\rm K}$. Since the present model galaxy has $n_{\rm p} \gtrsim 10^{-4}$ on average in high-temperature regions, we roughly suppose that all dust in high-temperature regions $(T \gtrsim 10^6 K)$ is evaporated by sputtering. Open triangles in the upper panel of Fig. 2 show the escape fractions when taking the sputtering into account. After including dust sputtering, $f_{\rm esc}=0.58$ at $t_{\rm age}=0.1$ Gyr, and $f_{\rm esc}=0.17$ at $t_{\rm age}=1.0$ Gyr. At higher redshifts, the dust sputtering somewhat enlarges the escape fractions, because a part of interstellar dust is distributed in high-temperature regions. On the other hand, at lower redshifts, the results are basically the same as no-sputtering cases, since ionizing photons are mainly absorbed by dust in low-temperature star-forming regions. Although the sputtering model here may overestimate the destruction of dust, the escape fractions do not change very much by including the dust sputtering. Also, in our simulations, the dust temperature does not rise over 100 K by photo-heating. Since the evaporation temperature of silicate dust is $\sim 10^3 \rm K$, the photodestruction of dust is unimportant.

In order to evaluate the relative escape fractions defined by (1), we make a mock observation of the simulated galaxy using the flux ratio at 1500 Å to 900 Å. Assuming $(L1500/L900)_{\rm int}=3$ (Steidel et al. 2001) and Q(1500 Å) = 1, and also that the radiation flux at 1500 Å is absorbed only by interstellar dust, we compute the transport of the radiation fluxes at 900 Å and 1500 Å. The resultant relative escape fractions $f_{\rm esc,rel}$ are shown by open squares in the lower panel of Fig. 2. It turns out that the predicted relative escape fractions ($f_{\rm esc,rel} \sim 0.1-0.3$) match the average of observed relative escape fractions as 0.14 (Shapley et al. 2006). Also, it is consistent with the observational estimates given by Steidel et al. (2001), Giallongo et al. (2002), and Inoue et al. (2005, 2006).

4 DISCUSSION

Shapley et al. (2006) estimated $f_{\rm esc,rel}$ for 14 LBGs in the SSA22a field, and they detected ionizing photons from only 2 LBGs, that is, C49 and D3. The reported relative escape fractions of 2 LBGs are extremely high as $f_{\text{esc,rel}}(\text{C49}) =$ 0.65, and $f_{\rm esc,rel}(D3) \ge 1.0$. For the other 12 LBGs, only upper limits are suggested. Iwata et al. (2009) reported the results of Subaru/Suprime-Cam deep imaging observations of the same field. They detected ionizing radiation from 7 LBGs as well as from 10 LAE candidates. They also showed the large scatter of the observed UV to Lyman continuum flux density ratios. For the seven detected LBGs, the ratio ranges from 2.4 to 23.8 with a median value of 6.6. Then, the relative escape fractions for 7 LBGs ranges from 0.03 to 0.30 after a correction for dust extinction, and can be 0.05-0.55if IGM extinction is taken into account. In addition, some of the detected galaxies show significant spatial offsets of ionizing radiation from non-ionizing UV emission.

The spatial distributions of interstellar dust are highly inhomogeneous in LAEs, because it should follow the inhomogeneous heavy-element distributions (see also Mori, Ferrara & Madau 2002; Mori, Umemura & Ferrara 2004). Therefore, the observed escape fractions strongly depend on viewing angles. We compute the probability distribution function, $dp(f)/df \equiv N(f)/N_{\text{total}}$, as a function of relative escape fraction along a line of sight, where $N_{\text{total}} = 128^2$ is the total number of bins in viewing angles and N(f) is the number of angular bins with a given escape fraction f. Figure 3 shows the probability distribution function from redshift $t_{\text{age}} = 0.1$ to 1.0 Gyr. This figure clearly shows that the relative escape fractions vary by viewing angles significantly. For example, depending on viewing angles, the relative escape fractions $f_{\rm esc,rel}$ vary from 0.18 to 0.43 at $t_{\text{age}} = 0.1$ Gyr and from 0.12 to 0.47 at $t_{\text{age}} = 1.0$ Gyr. These probability distributions are indicated by a pink belt in the lower panel of Fig. 2. The standard deviation at each

6

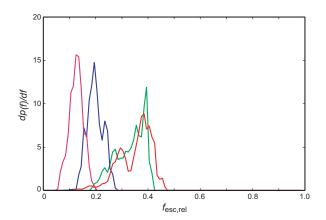


Figure 3. Probability distribution of relative escape fractions. Each line corresponds to the probability distribution at $t_{\rm age} = 0.1 \, {\rm Gyr}$ (green), 0.3 Gyr (blue), 0.3 Gyr (magenta) and 1.0 Gyr (red), respectively.

redshift is also shown by a red belt. This effect allows some of observed LAEs and LBGs to have as high escape fraction as reported by Iwata et al. (2009).

The present analyses show the absolute escape fractions $f_{\rm esc}$ for LAEs and LBGs can be as large as $f_{\rm esc}\gtrsim 0.17$. Hence, LAEs and LBGs are potential sources for the IGM ionization at $z\gtrsim 4$. Here, we quantify the contributions of LAEs and LBGs to the IGM ionization. Specifically, we assess the emission rate of ionizing photons from LAEs and LBGs per unit comoving volume. The emission rate is evaluated from the star formation rate based on the observed luminosity functions, with coupling the escape fractions for LAE and LBG phases obtained in the present analysis. We use the average escape fraction $< f_{\rm esc} >= 0.35$ for the LAE phase and $< f_{\rm esc} >= 0.18$ for the LBG phase.

In Figure 4, the emission rate of ionizing photons per comoving Mpc³ is shown as a function of redshift. Open symbols depict the emission rate for the samples of LAEs that listed in the caption. Filled symbols show the emission rate for LBGs, which is estimated by extrapolating the luminosity function to $L = 0.1L_{z=3}^*$ from Steidel et al. (1999) with dust extinction of E(B-V)=0.13(see also Yoshida et al. 2006). As a theoretical criterion, we adopt that by Madau, Haadt & Rees (1999), where the emission rate of ionizing photons required to balance the recombination is given by $\dot{N}_{\text{ion}} = 10^{47.4} C(1+z)^3 \text{ s}^{-1} \text{Mpc}^{-3}$. C is the clumping factor which parameterizes the inhomogeneity of ionized hydrogen in the IGM. Madau et al. (1999) adopted C = 30, based on the value computed by a cosmological radiative transfer simulation of Gnedin & Ostriker (1997). Ouchi et al. (2004) also adopted C=30 when computing the number of ionizing photons needed to keep the IGM highly ionized at z = 5, as do a number of other authors. Although C may have some uncertainty, we assume C=30 here as a fiducial value.

Figure 4 clearly illustrates that observed LBGs can provide the majority of ionizing photons at z=3-5, and play an important role to keep the universe ionized. However, LAEs are not capable of ionizing large volumes at the redshift z=3-5. On the other hand, ionizing photons

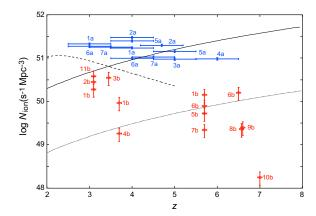


Figure 4. The evolution of emission rate of ionizing photons per comoving Mpc, $\dot{N}_{\rm ion}$, as a function of redshift. Open symbols represent $\dot{N}_{\rm ion}$ of LAEs derived from 1a) Ouchi et al. (2008), 2a) Kudritzki et al. (2000), 3a) van Breukelen, Jarvis & Venemans (2005), 4a) Fujita et al. (2003), 5a) Ajiki et al. (2003), 6a) Malhotra & Rhoads (2004), 7a) Rhoads et al. (2003), 8a) Kodaira et al. (2003), 9a) Taniguchi et al. (2005), 10a) Iye et al. (2006), and 11a) Gronwall et al. (2007) with $\langle f_{\rm esc} \rangle =$ 0.35 which is mean escape fraction at LAE phase. The blue filled symbols represent the $\dot{N}_{\rm ion}$ of LBGs derived from 1b) Steidel et al. (1999), 2b) Yoshida et al. (2006), 3b) Iwata et al. (2003), 4b) Bouwens et al. (2006), 5b) Ouchi et al. (2004), 6b) Sawicki & Thompson (2006), and 7b) Gabasch et al. (2004) with $\langle f_{\rm esc} \rangle = 0.18$ which is mean escape fraction at LBG phase. The horizontal and vertical error-bars are arisen from the uncertainty of observations and the variation of escape fractions (LAE: $f_{\rm esc} = 0.22 - 0.47$, LBG: $f_{\rm esc} = 0.17 - 0.19$), respectively. A solid line and a dotted line indicate the emission rate required to ionize the IGM with C=30 and C=1, respectively (Madau et al. 1999). A dashed line represents the emission rate evaluated by the QSO luminosity function.

from not only LBGs but also LAEs are not enough to ionize the IGM at $z\gtrsim 6$. Most of photons that ionize the universe may come from undetected faint LAEs and LBGs or other sources. Recently, Choudhury & Ferrara (2007) studied the cosmic reionization history to account for a number of observational data, and pointed out that low-mass galaxies hosting Pop III stars can be predominant ionizing sources of the IGM at high-z. Our results advocate their model. In the present analysis, all Lyman α photons are assumed to escape. Hence, the contribution of LAEs may be underestimated. In the future work, we intend to include Lyman α line transfer to compare the numerical results more precisely with the observations.

5 SUMMARY

We have performed three-dimensional radiation transfer calculations, based on a high-resolution hydrodynamic simulation of a supernova-dominated primordial galaxy, to obtain the ionization structure and explore the escape fractions of ionizing photons from LAEs and LBGs at high redshifts. The effect of dust extinction is incorporated according to the chemical enrichment, taking the size distributions of dust into account. As a result, we find that dust extinction reduces the escape fractions by a factor of 1.5-8.5 in the LAE phase and by a factor of 2.5-11 in the LBG

phase. The resultant escape fractions are 0.07 - 0.47 in the LAE phase and 0.06 - 0.17 in the LBG phase. These results are well concordant with recent observations. We have found that the combination of diffuse distributions of stars and supernova shock-heating is important for UV escape fractions. In the present galaxy model, young stars are extendedly distributed, and also the bulk of interstellar gas is collisionally ionized by supernova shock-heating. Since the interstellar medium is moderately optically-thin and quite bubbly, ionizing photons can escape through collisionally-ionized regions. The collisional ionization by shocks contributes by a factor of ≈ 2 to the increase of the escape fractions.

The relative escape fractions derived by mock observations of the simulated galaxy match quite well the estimates by recent observations for LAEs and LBGs. To assess the contribution of LAEs and LBGs to the IGM ionization, the resultant escape fractions have been combined with the luminosity functions of LAEs and LBGs. As a result, we find that high-z LAEs and LBGs can ionize the IGM at z = 3-5. However, ionizing radiation from LAEs as well as LBGs is not enough to ionize the IGM at z > 6. That implies that undetected faint LAEs and LBGs or additional ionization sources may determine the IGM ionization at z > 6.

Very recently, Wise & Cen (2009) performed 3D radiation hydrodynamic simulations to assess the contribution of dwarf galaxies to cosmic reionization at redshift z = 8. They studied the UV escape fractions for low-mass galaxies in the mass range of $M_{\text{total}} = 3 \times 10^6 - 3 \times 10^9 M_{\odot}$. As a result, they have shown that the UV escape fractions can reach up to \sim 0.8 without dust extinction in halos with $> 10^8 M_{\odot}$ for a top-heavy initial mass function (IMF). However, in order to assess the contribution of LAEs and LBGs to IGM reionization, we should evaluate the UV escape fractions from more massive galaxies with dust extinction. Here, we have shown that a high-mass, metal-enriched galaxy at low redshifts can allow escape fractions as large as some tens per cent . We have found that an order-of-magnitude increase in the escape fractions can be attributed to the diffuse distribution of stars, while the collisional ionization further raises them by some factor.

ACKNOWLEDGMENTS

We are grateful to A. Inoue, A. Ferrara, and A. Razoumov for valuable discussion and comments. Numerical simulations have been performed with the FIRST simulator and T2K-Tsukuba at Center for Computational Sciences, in University of Tsukuba. This work was supported in part by the FIRST project based on Grants-in-Aid for Specially Promoted Research by MEXT (16002003) and JSPS Grant-in-Aid for Scientific Research (S) (20224002), (A) (21244013), and (C) (18540242).

REFERENCES

Ajiki M. et al., 2003, AJ, 126, 2091 Alvarez M. A., Bromm V., Shapiro P. R., 2006, ApJ, 639,

Arimoto N., Yoshii Y., 1987, A&A, 173, 23

Bouwens R. J., Illingworth G. D., Blakeslee J. P., Franx M., 2006, ApJ, 653, 53

Bouwens R. J., Illingworth G. D., Franx M., Ford H., 2007, ApJ, 670, 928

Bukner A. J., Stanway, E. R., Ellis, R. S., McMahon, R. G., 2004, MNRAS, 355, 374

Choudhury T. R., Ferrara A., 2007, MNRAS, 380, L6

Ciardi B., Bianchi S., Ferrara A., 2002, MNRAS, 331, 463

Cowie L. L., Hu E. M., 1998, AJ, 115, 1319

Draine B. T., Lee H. M., 1984, ApJ, 285, 89

Draine B. T., Salpeter E. E., 1979, ApJ, 231, 77

Dunkley J. et al., 2009, ApJS, 180, 306

Fan, X. et al., 2001, AJ, 122, 2833

Fan X., et al., 2006, AJ, 132, 117

Fioc M. Rocca-Volmerange B., 1997, A& A, 326, 950

Fujita S. S. et al., 2003, AJ, 125, 13

Gabasch A. et al., 2004, A& A, 421, 41

Giallongo E., Cristiani S., D'Odorico S., Fontana A., 2002, ApJ, 568, L9

Gibson B. K., 1997, MNRAS, 290, 471

Gnedin N. Y., 2008, ApJ, 673, L1

Gnedin N. Y. Ostriker, J. P., 1997, ApJ, 486, 581

Gnedin N. Y., Kravtsov, A. V., Chen, H.-W., 2008, ApJ, 672, 765

Gronwall C. et al., 2007, ApJ, 667, 79

Haardt, F., Madau, P., 1996, ApJ, 461, L20

Inoue A. K., Iwata I., Deharveng J.-M., Buat V., Burgarella D., 2005, A& A, 435, 471

Inoue A. K., Iwata I., Deharveng J.-M., 2006, MNRAS, 371, L1

Iliev I. T. et al., 2006a, MNRAS, 371, 1057

Iwata I. et al., 2003, PASJ, 55, 415

Iwata I. et al., 2009, ApJ, 692, 1287

Ive M. et al., 2006, Nature, 443, 186

Kawata D., Gibson B. K., 2003, MNRAS, 340, 908

Kawata D., Gibson B. K., 2003, MNRAS, 346, 135

Kitayama T., Yoshida N., Susa H., Umemura M., 2004, ApJ, 613, 631

Kodaira K. et al., 2003, PASJ, 55, L17

Kodama T., Arimoto N., 1997, A&A, 320, 41

Kudritzki R. -P. et al., 2000, ApJ, 536, 19

Madau P., Haardt F., Rees M. J., 1999, ApJ, 514, 648

Malhotra S., Rhoads J. E., 2004, ApJ, 617, L5

Mannucci F. et al., MNRAS in press (arXiv:0902.2398)

Mathews W. G., Brighenti F., 2003, ApJ, 590, L5

Mathis J. S., Rumpl W., Nordsieck K. H., 1977, ApJ, 217, 425

Mori M., Umemura M., 2006, Nature, 440, 644

Mori M., Ferrara A., Madau P., 2002, ApJ, 571, 40

Mori M., Umemura M., Ferrara A., 2004, ApJ, 613, L97

Nakamoto T., Umemura M., Susa H., 2001, MNRAS, 321,

Osterbrock D. E., 1989, "Astrophysics of Gaseous Nebulae and Active Galactic Nuclei" (University Science Books)

Ouchi M. et al., 2004, ApJ, 611, 660

Ouchi M. et al., 2008, ApJS, 176, 301

Page L. et al., 2007, ApJS, 170, 335

Pettini M. et al., 2001, ApJ, 554, 981

Razoumov A. O., Sommer-Larsen J., 2006, ApJ, 651, L89

Razoumov A. O., Sommer-Larsen J., 2007, ApJ, 668, 674

Rhoads J. E. et al., 2003, AJ, 125, 1006 Salpeter E. E., 1955, ApJ, 121, 161 Sawicki M., Thompson D., 2006, ApJ, 642, 653 Shapley A. E., Steidel C. C., Pettini M., Adelberger K. L., Erb D. K., 2006, ApJ, 651, 688 Steidel C. C., Adelberger K. L., Giavalisco M., Dickinson M., Pettini M., 1999, ApJ, 519, 1

Steidel C. C., Pettini M., Adelberger K. L., 2001 ApJ, 546, 665
Susa H., Umemura M., 2000, ApJ, 537, 578
Susa H., Umemura M., 2004, ApJ, 600, 1
Taniguchi Y. et al., 2005, PASJ, 57, 165
Thoul A. A., Weinberg D. H., 1996, ApJ, 465, 608
Tsai J. C., Mathews W. G., 1995, ApJ, 448, 84
Umemura M., Ikeuchi S., 1984, PThPh, 72, 47

Umemura M., Nakamoto T., Susa H., 2001, ASPC, 222, 109

van Breukelen C., Jarvis M. J., Venemans B. P. 2005, MN-RAS, 359, 895

Whalen D., Abel T., Norman M. L., 2004, ApJ, 610, 14 Wise J. H., Cen R., 2009, ApJ, 693, 984 Yoshida M. et al., 2006, ApJ, 653, 988